Supporting information

High Surface Area Siloxene for Photothermal and Electrochemical Catalysis

Yize Su,‡[a] Shenghua Wang,‡[a] Liang Ji,‡[a] Chengcheng Zhang,[a] Haiting Cai,[b] Hui Zhang[a] and Wei Sun*[a]

[a]State Key Laboratory of Silicon Materials, School of Materials Science and Engineering, Zhejiang University, Hangzhou, Zhejiang 310027, P. R. China.

[b]Institute of Industrial Catalysis, College of Chemical Engineering, Zhejiang University of Technology, Hangzhou 310014, China

‡These authors contributed equally to this work.

*Corresponding author: Wei Sun

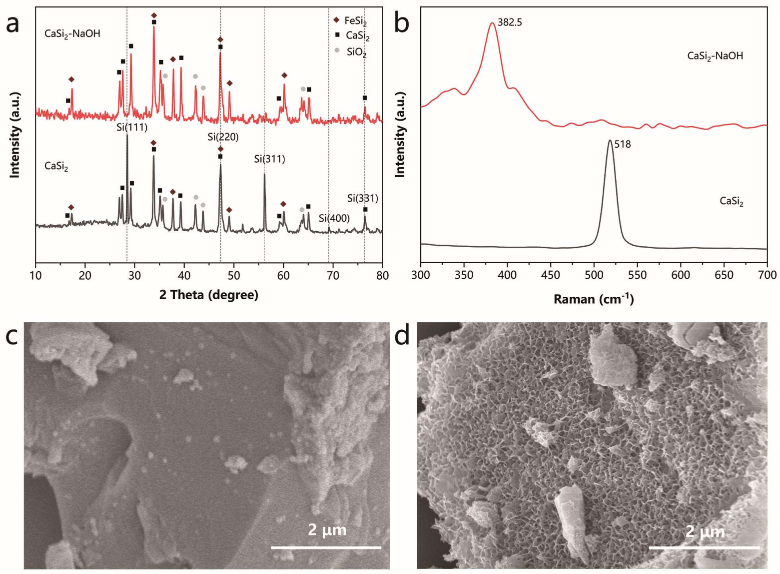

Fig. S1 (a) XRD patterns of $CaSi_2$ and $CaSi_2$-NaOH. The peaks are labelled according to the standard SiO_2, the standard Si, the standard $FeSi_2$ and the standard $CaSi_2$. Subtle peaks of $FeSi_2$ and SiO_2 could be observed in the pattern, but all of them were far less pronounced than the Si peaks. (b) Raman spectra of $CaSi_2$ and $CaSi_2$-NaOH. (c) SEM image of $CaSi_2$. (d) SEM image of $CaSi_2$-NaOH.

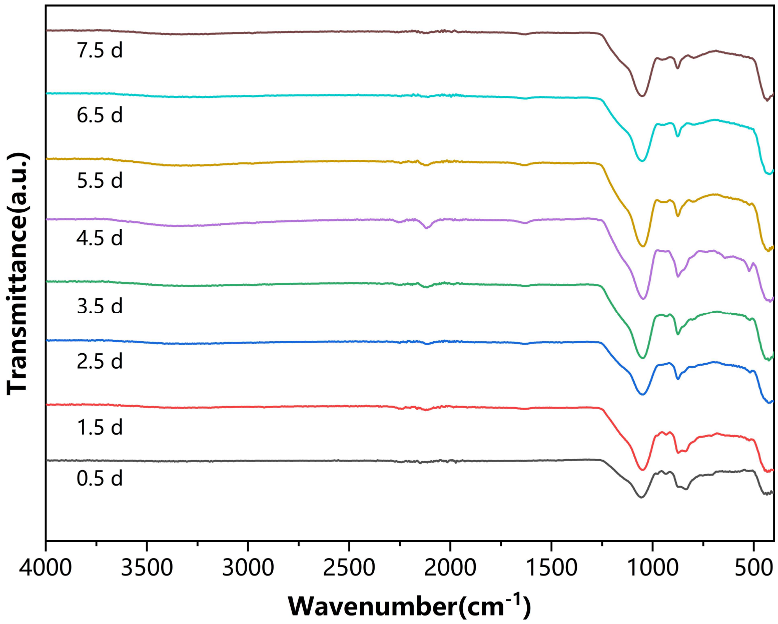

Fig. S2 FTIR spectra of siloxene prepared with different reaction time.

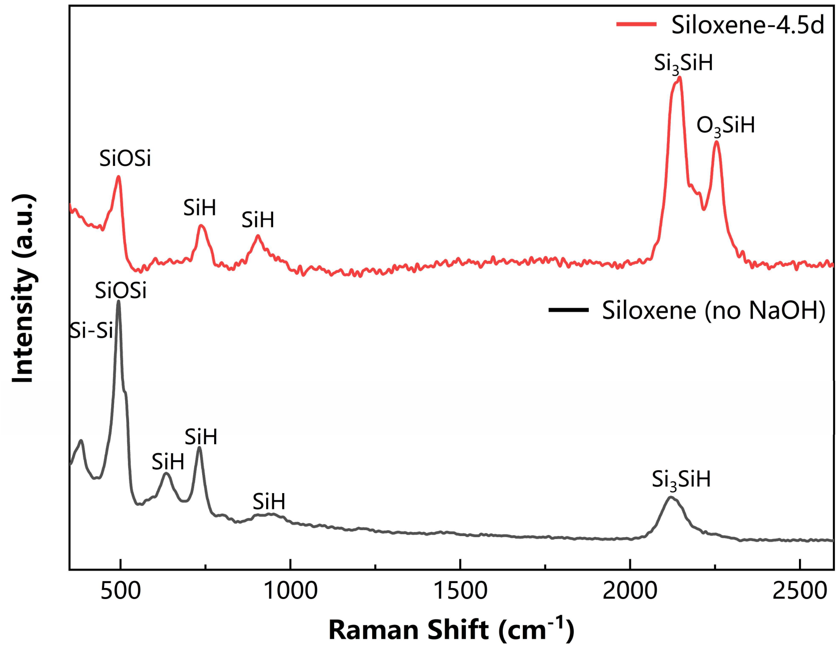

Fig. S3 Raman spectra of siloxene-4.5d and siloxene (no NaOH).

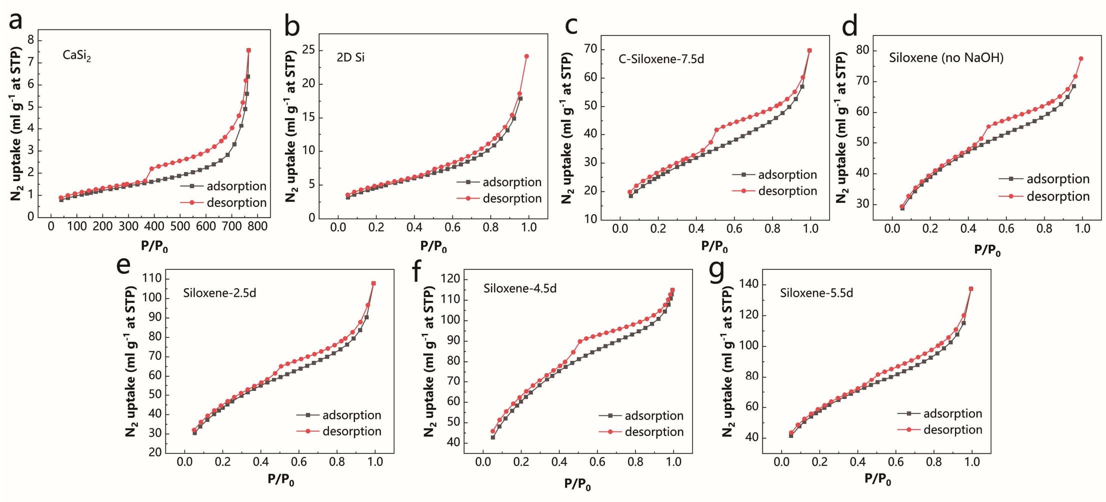

Fig. S4 N_2 adsorption-desorption isotherms of (a) $CaSi_2$, (b) 2DSi, (c) C-siloxene-7.5d, (d) siloxene (no NaOH), (e) siloxene-2.5d, (f) siloxene-4.5d, and (g) siloxene-5.5d.

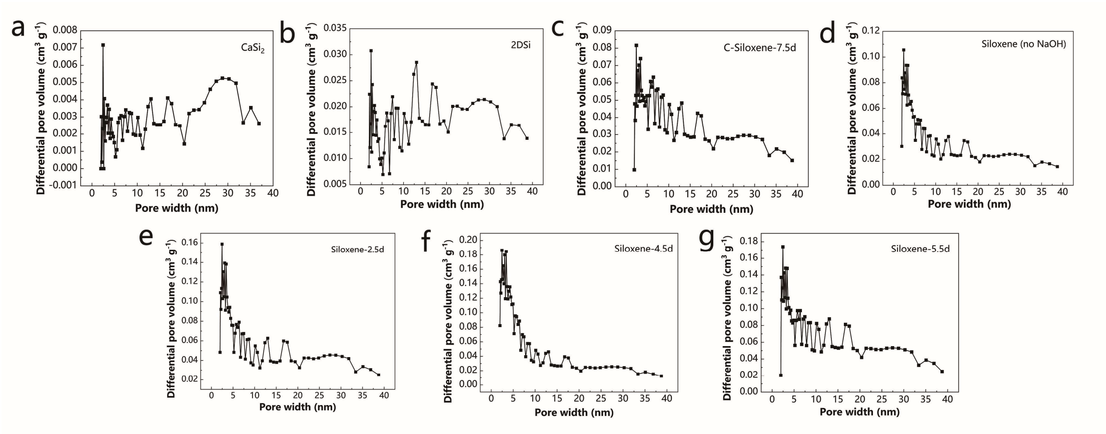

Fig. S5 Pore size distribution curves of (a) $CaSi_2$, (b) 2DSi, (c) C-siloxene-7.5d, (d) siloxene (no NaOH), (e)siloxene-2.5d, (f) siloxene-4.5d, and (g) siloxene-5.5d.

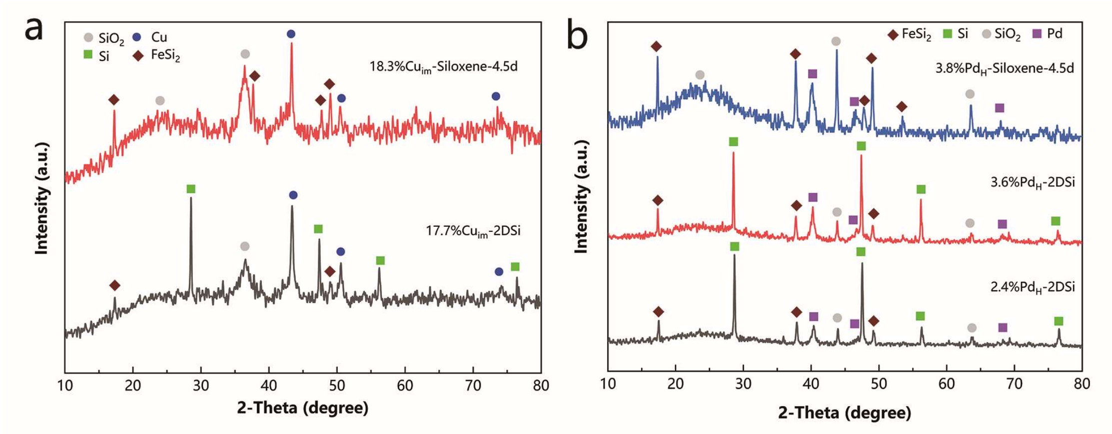

Fig. S6 (a) XRD patterns of 17.7%Cu_{im}-2DSi and 18.3%Cu_{im}-Siloxene-4.5d. (b) XRD patterns of 2.4%Pd_H-2DSi, 3.6%Pd_H-2DSi and 3.8%Pd_H-Siloxene-4.5d. The peaks are labelled according to the standard SiO_2, the standard Si, the standard $FeSi_2$, the standard Cu, and the standard Pd.

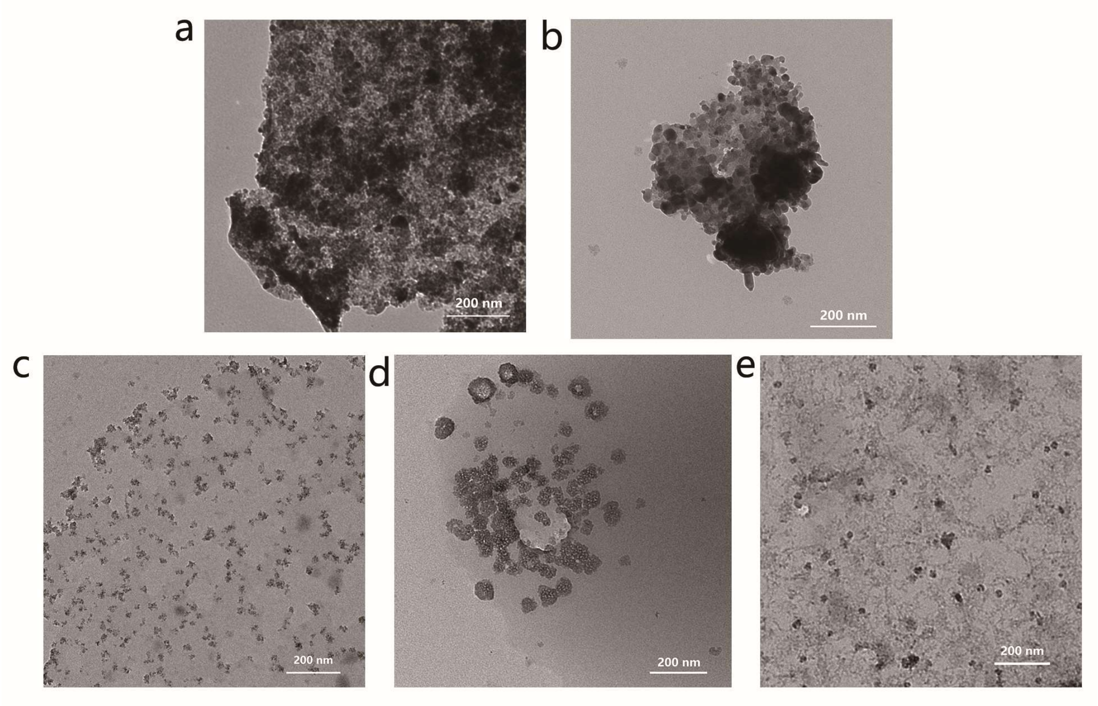

Fig. S7 TEM images of (a) 17.7%Cu_{im}-2DSi, (b) 18.3%Cu_{im}-Siloxene-4.5d, (c) 2.4%Pd_H-2DSi, (d) 3.6%Pd_H-2DSi, and (e) 3.8%Pd_H-Siloxene-4.5d.

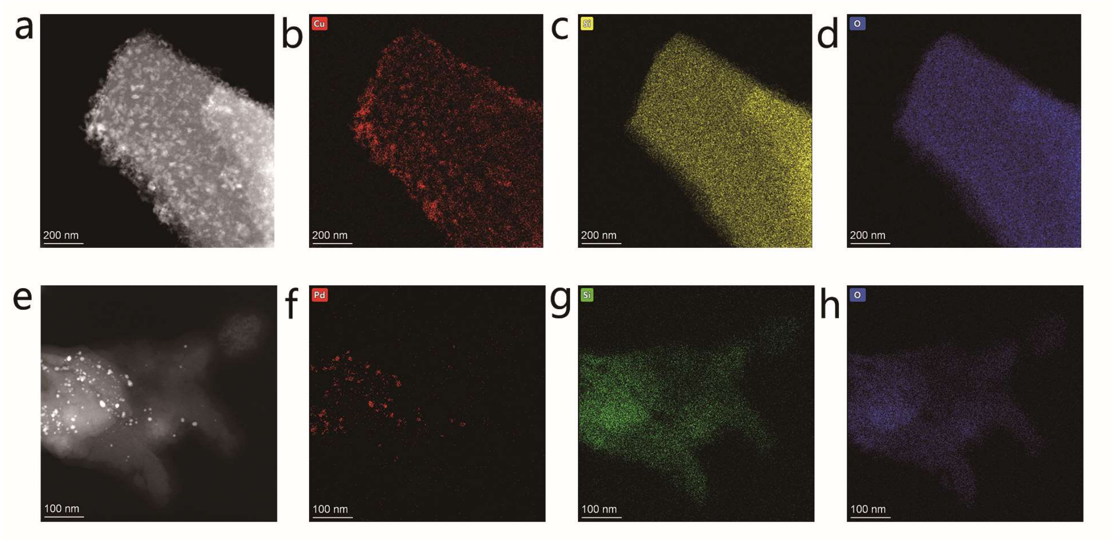

Fig. S8 EDS mappings of (a-d) 18.3%Cu_{im}-siloxene-4.5d and (e-h) 3.8%Pd_H-siloxene-4.5d.

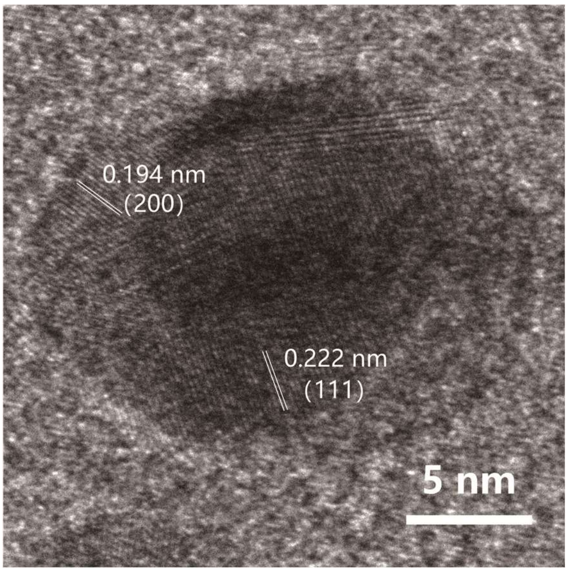

Fig. S9 HRTEM image of 3.8%Pd_H-siloxene-4.5d.

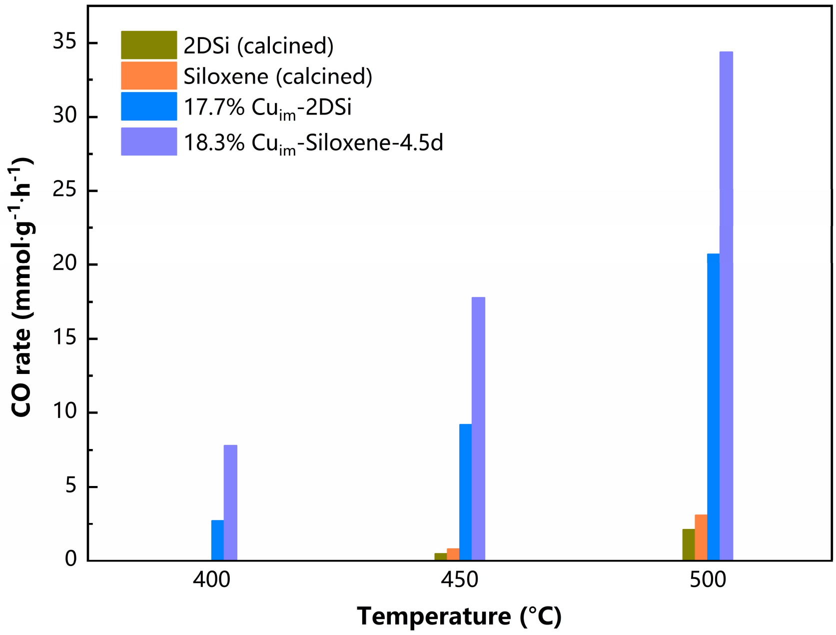

Fig. S10 CO production rates of different samples in thermocatalytic reactions (testing condition: 30 mg of the catalyst, $CO_2/H_2/N_2 = \sim 5/20/5$, ambient pressure).

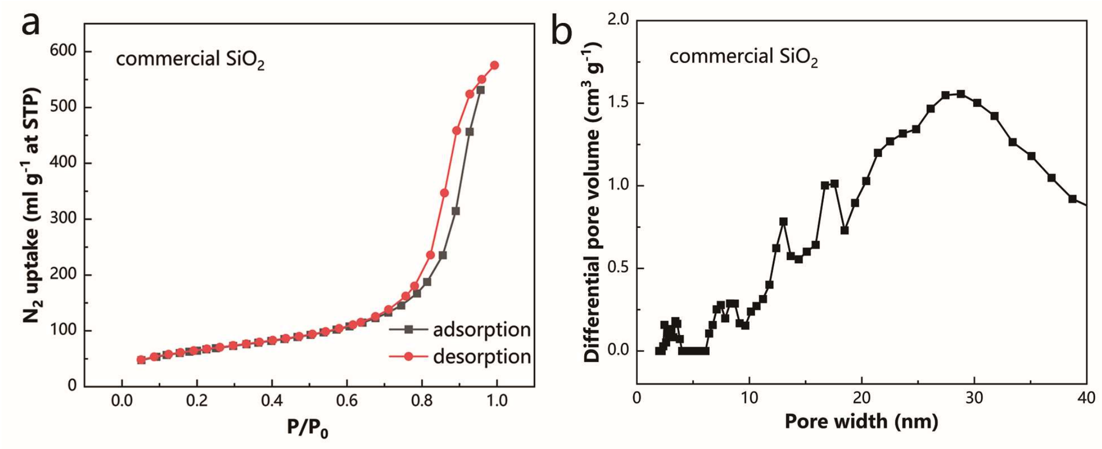

Fig. S11 (a) N_2 adsorption-desorption isotherms and (b) pore size distribution curves of commercial SiO_2.

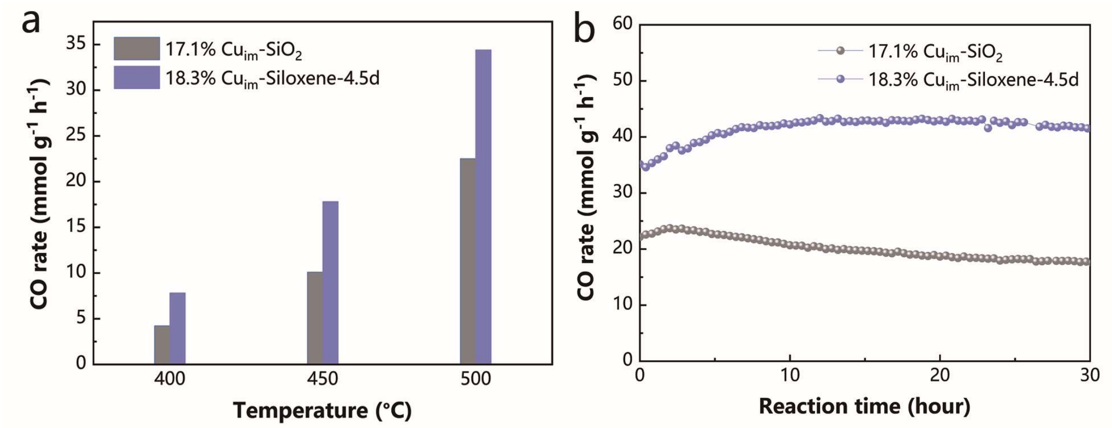

Fig. S12 CO production rates of 17.1%Cu_{im}-SiO_2 and 18.3%Cu_{im}-siloxene-4.5d in thermal catalytic reactions (testing condition: 30 mg of the catalyst, $CO_2/H_2/N_2$ = ~5/20/5, ambient pressure).

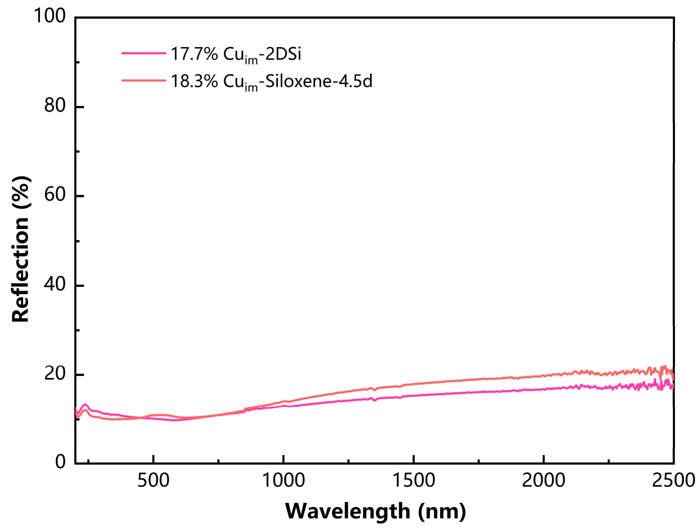

Fig. S13 Diffuse reflectance spectra of 17.7%Cu$_{im}$-2DSi and 18.3%Cu$_{im}$-Siloxene-4.5d.

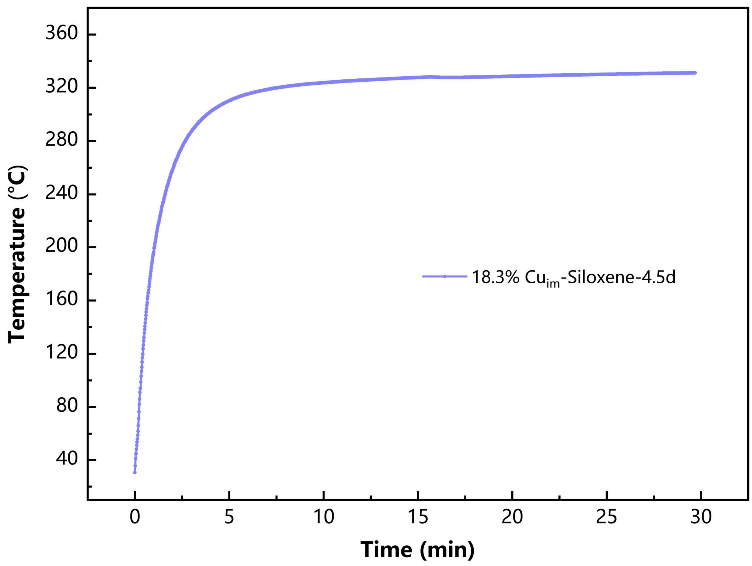

Fig. S14 Surface temperature profile of 18.3%Cu_{im}-Siloxene-4.5d under 34.3-suns illumination.

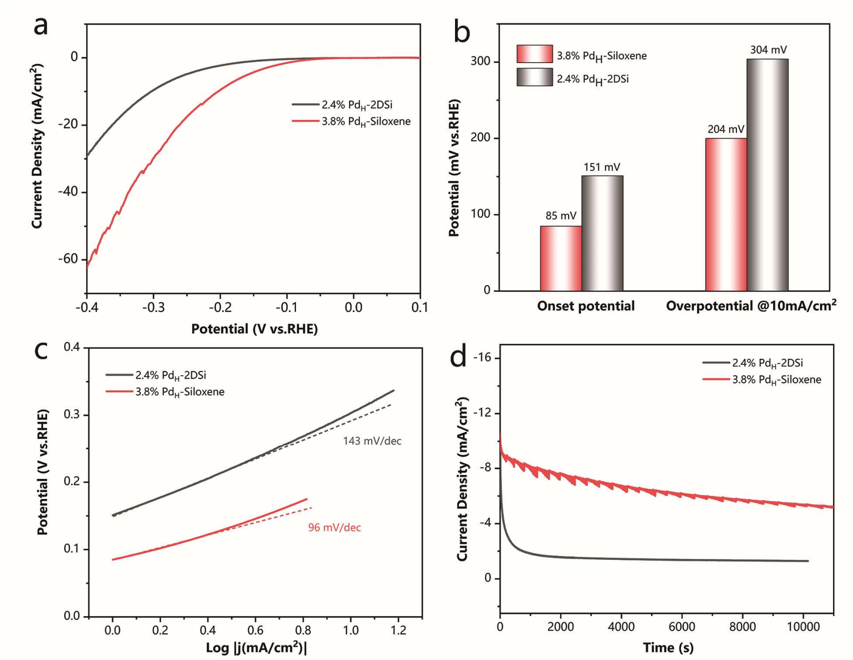

Fig. S15 (a) Polarization curves of the 2.4% Pd_H-2DSi and 3.8% Pd_H-siloxene-4.5d catalysts. (b) Comparison of overpotential at 10 mA/cm^2 and onset potential of the catalysts. (c) Tafel plots of the catalysts. (d) chronoamperometry tests of the catalysts.

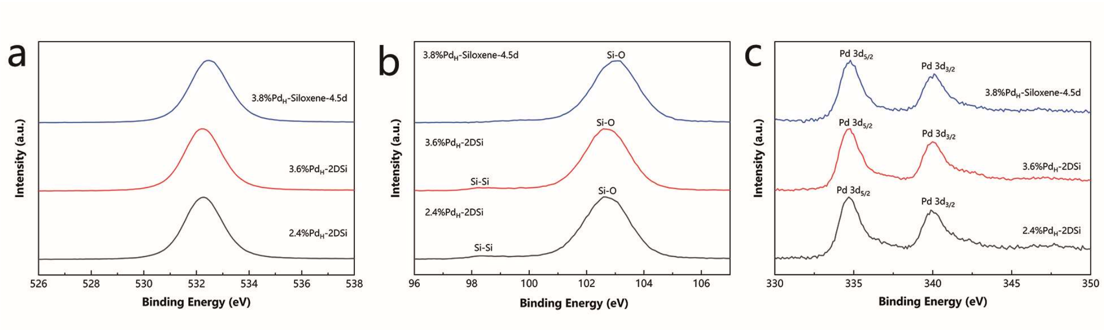

Fig. S16 (a) O 1s, (b) Si 2p, and (c) Pd 3d XPS spectra of the different Pd catalysts.

Table S1 Crystallite size of the metals in different samples estimated using the Scherrer Equation based on the XRD patterns.

Samples	18.3%Cu_{im}-Siloxene-4.5d	17.7%Cu_{im}-2DSi	3.8%Pd_H-Siloxene-4.5d	3.6%Pd_H-2DSi	2.4%Pd_H-2DSi
Metallic crystallite size (nm)	9	11	11	17	13

Table S2 CO rates of different samples in photothermal catalytic reactions (testing condition: 15 mg of the catalyst, $CO_2/H_2/N_2$ = ~2.5/10/2.5, ambient pressure).

Light Illumination (suns)	17.7%Cu_{im}-2DSi	15.9%Cu_{im}-Siloxene (no NaOH)	18.3%Cu_{im}-Siloxene
20.0	0.000	0.628	1.245
24.2	0.483	0.875	3.040
34.3	1.898	3.818	8.403